Computer vision on color-band resistor and its cost-effective diffuse light source design

Article *in* Journal of Electronic Imaging · July 2016

DOI: 10.1117/1.JEI.25.6.061409

The following manuscript was published in

Yung-Sheng Chen and Jeng-Yau Wang, "**Computer vision on color-band resistor and its cost-effective diffuse light source design**," *Journal of Electronic Imaging*, Vol. 25, No. 6, 061409 (16 pages), 2016. https://dx.doi.org/10.1117/1.JEI.25.6.061409

Computer vision on color-band resistor and its cost-effective diffuse light source design

Yung-Sheng Chen,[a,*] Jeng-Yau Wang[a,b]
[a]Yuan Ze University, Department of Electrical Engineering, 135 Yuan-Tung Road, Chung-Li, Taoyuan 320, Taiwan, ROC
[b]National Chung-Shan Institute of Science and Technology, System Development Center, Lung-Tung, Taoyuan 325, Taiwan, ROC

Abstract. Color-band resistor possessing specular surface is worthy of studying in the area of color image processing and color material recognition. The specular reflection and halo effects appearing in the acquired resistor image will result in the difficulty of color band extraction and recognition. In this paper, a computer vision system is proposed to detect the resistor orientation, segment the resistor's main body, extract and identify the color bands, as well as recognize the color code sequence and read the resistor value. The effectiveness of reducing the specular reflection and halo effects are confirmed by several cheap covers, e.g., paper bowl, cup or box inside pasted with white paper combining with a ring-type LED controlled automatically by the detected resistor orientation. The calibration of microscope used to acquire the resistor image is described and the proper environmental light intensity is suggested. Experiments are evaluated by 200 4-band and 200 5-band resistors comprising 12 colors used on color-band resistors, and show the 90% above correct rate of reading resistor. The performances reported by the failed number of horizontal alignment, color band extraction, color identification, as well as color code sequence flip over checking confirm the feasibility of the presented approach.

Keywords: Color-band resistor, computer vision, diffuse light source, image processing, image segmentation.

***Yung-Sheng Chen, E-mail: eeyschen@saturn.yzu.edu.tw

1 Introduction

Computer vision has widely influenced our daily life, in particular, the color camera used in the industrial and commercial fields for object segmentation and recognition.[1,2] Light sources play a significant role to acquire a qualified image from objects for facilitating the image processing and pattern recognition. For objects possessing specular surface, the phenomena of reflection and halo appearing in the acquired image will increase the difficulty of information processing. Such a situation may be improved by the assistance of applicable diffuse light source.[3] In this paper, the color-band resistor possessing specular surface is studied for designing a cost-effective diffuse light source and developing a computer vision system to read the resistor value.

Color band resistors are widely used in electrical/electronic circuits and products and often divided into two types: 4-band (R_4) and 5-band (R_5) resistor. Twelve colors are selected to print on the color bands depending on the representative resistor value. Reading color-band resistor value is normally performed by eyes for color identification and calculation with color code mapping as listed in Table 1. In rule, reading the resistor value of R_4 and R_5 can be computed respectively by Eq. (1) and Eq. (2), where C_i, M, and τ denote the i-th color code, multiplier, and tolerance, respectively. In normal color band sequence, the color band of tolerance should be at the right-most side. If a 5-band resistor is aligned horizontally and the colored band of tolerance is at right for instance, then the sequence of the five colored bands from left to right will be C_1, C_2, C_3, M, and τ. The value of R_5 is thus computed based on Eq. (2).

$$R_4 = M\left(\sum_{i=1}^{2} 10^{2-i} C_i\right) \pm \tau \tag{1}$$

$$R_5 = M\left(\sum_{i=1}^{3} 10^{3-i} C_i\right) \pm \tau \tag{2}$$

Table 1 Mapping a resistor color band into color code, multiplier, and tolerance. Here "-" denotes "Not Available".

Color (code)	C_1	C_2	C_3	M	τ
Black (0)	-	0	0	10^0	-
Brown (1)	1	1	1	10^1	1%
Red (2)	2	2	2	10^2	2%
Orange (3)	3	3	3	10^3	-
Yellow (4)	4	4	4	10^4	-
Green (5)	5	5	5	10^5	0.5%
Blue (6)	6	6	6	10^6	0.25%
Violet (7)	7	7	7	10^7	0.1%
Gray (8)	8	8	8	-	0.05%
White (9)	9	9	9	-	-
Gold (10)	-	-	10	10^{-1}	5%
Silver (11)	-	-	11	10^{-2}	10%

Except for the use of multimeter, the significant information for reading a color-band resistor can be based on the color information and the color code sequence. It is not easily or impossibly

read by an electronic engineer with color-blindness,[1,2] poor eyesight, or a non-professional person. Therefore, it is a valuable work for developing a computer vision system that can read resistor values. Chan and Wang developed a non-contact approach to reading the resistor value, in which they reported that the CIE-LAB color space can exhibit good properties for color recognition task and discussed the Bayes classifier and predefined color region method for color identification.[4] However, how to setup the resistor for image acquisition and segment color bands in a resistor are unknown. The method presented by Mitani, Sugimura, and Hamamoto focused merely on the case of well-aligned (i.e., the resistor has been aligned horizontally with normal color band sequence beforehand) 4-band resistor without considering the silver color.[5] In addition, Mitani and Hamamoto used their method[5] to investigate the performance of reading resistor's colors with 10 color feature models and recommended the $L^*u^*v^*$ color space for the application.[6] From these results, five issues remained as follows are addressed in this paper to propose a total solution for dealing with them. First, the light source should be considered since the carbon film and metal film color-band resistors have highly specular reflective surface which is unfavorable to image processing and color identification. Other difficulties may also include non-uniform intensity, variation in coating pigments, color spread, and spectral response of the CCD camera as described in Ref. 4. Secondly, from the practical viewpoint, the resistor should be placed in any location and orientation within the image acquired range, and can be located precisely. Thirdly, the color bands should be automatically extracted even though it is a difficult task as mentioned in Ref. 5. Fourthly, since there are 12 colors used in the 4-band and 5-band resistors, all the colors should be considered in the color identification. Note here that inconsistencies of colors in the stripe ink in 4-band and 5-band resistor leading to color

identification more complex should be overcome. Finally, the sequence of color bands (or color codes) should be analyzed for computing the resistor value since the reverse sequence is possible.

Except for the resistor image researches mentioned previously,[4-6] some other related works are described as follows. In our study, the segmentation of resistor image using ISH (intensity/saturation/hue) colour space is first mentioned by Claxton and Kwok.[7] Benchoff introduced an app of Android resistor scanner made by D. Parth for 4-band resistor recognition.[8] The image may shake severely causing it hard to aim the scanning line at resistor body especially at zoom situation. There is also an iOS/iPhone app for optical recognition of resistor codes,[9] which needs the user to drag ROI on the color bands like to aim the scanning line at resistor body. As one of our goals, the resistor recognition system should be easy to use without bothering user to drag any ROI or to aim scanning line on the resistor image. In the recent past, to achieve this goal and overcome the five issues mentioned previously, we have primarily presented partial works on image processing algorithms[10] and investigation on diffuse light sources[11] for reading resistor. After completing the whole system and the performance evaluation, the details of our design are reported in this paper.

The rest of this paper is organized as follows. In Sec. 2, the whole system is described, where the configuration of ring-type LED light source is also presented. Section 3 presents the details of the developed algorithms for processing resistor image, which mainly include (1) thresholding and horizontal alignment, (2) segmentation of resistor's main body, (3) color band extraction, (4) color identification, as well as (5) sequence analysis of color codes. The experimental results and discussions are given in Sec. 4, where the effectiveness of different cost-effective paper domes is also reported. The conclusion is finally drawn in Sec. 5.

2 System Description

To study the color bands on a resistor with reflective surface, two subjects are considered in this paper. One is to segment and identify the color band as well as recognize the resistor by means of image processing algorithms. The other is to reduce the specular reflection and halo effects by means of cost-effective diffuse light source design for effectively processing the considered resistor image. Figure 1 shows the block diagram of the developed system. Except that the image processing algorithms are implemented in a personal computer (PC) and will be detailed in next section, the diffuse light source including replaceable paper dome and controllable light source can be manipulated automatically via a feedback mechanism. Once a resistor on the sliding table is sent to the defined position under the paper dome combining a USB microscope, the microscope will capture the initial resistor image into the PC to determine the resistor orientation. Based on the detected resistor orientation, the light source will be controlled properly and combined with the paper dome for taking the final resistor image which the specular reflection and halo effects have been reduced. In this study, the sliding table and light source are controlled by Arduino Mega 2560 microcontrollers.[12] In addition, to facilitate the system integration and build the user interface the proposed algorithms are implemented in LabVIEW environment combining with the MATLAB codes. The acquired image is of 640×480 pixels.

Except for the replaceable paper dome, our light source is designed by a 24-LED ring-type structure as illustrated in Fig. 2. The on/off of LEDs are controlled automatically based on the detected orientation of the resistor. The dimming of LED is based on PWM (pulse width modulation) technique[13,14] for determining the luminous intensity, where its proper range for our experiments will be reported in Sec. 4.3. To further reduce the specular reflection, only the 5-LED near each wire terminal of the resistor will be turned on and the others turned off. For

example, the LED 22, 23, 0, 1, 2 as well 10, 11, 12, 13, 14 are turned on while the detected resistor orientation (θ_{dro} with degree unit) is near to zero degree as illustrated in Fig. 2. In the ring-type structure, there are 24 LEDs arranged in 360°, where one LED is allocated within 15°. Moreover since the θ_{dro} is within 180°, an index $\hat{I}$, the integral part of dividing θ_{dro} by 15, is used to control the LEDs. The set $S_{LED-on}(\hat{I})$ of turned on LEDs indexed by $\hat{I}$ may be expressed as below

$$S_{LED-on}(\hat{I}) = \bigcup_{k=0}^{1} \bigcup_{i=-2}^{2} LED_{(24+12k+\hat{I}+i)\%24} \qquad \text{where } \hat{I} = \text{Int}\left(\frac{\theta_{dro}}{15}\right). \tag{3}$$

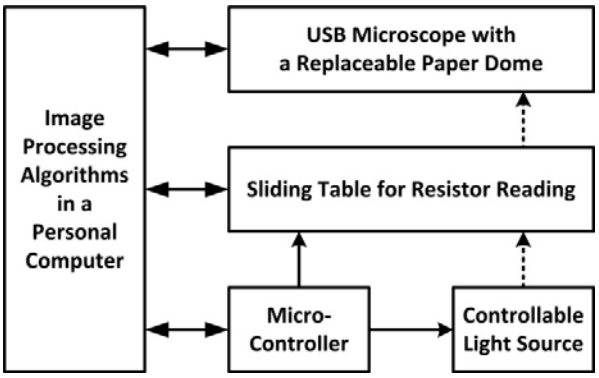

Fig. 1 Block diagram of the developed system.

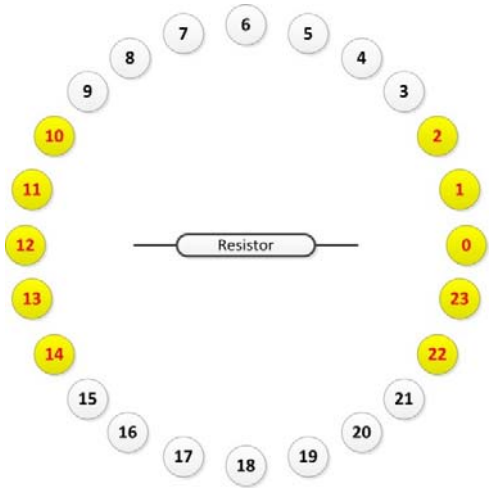

Fig. 2 Light source designed by a controllable 24-LED ring-type structure. In this illuatration, $S_{LED-on}(0) = \{22, 23, 0,1,2,10,11,12,13,14\}$ while the $\theta_{dro} = 0°$.

3 Proposed Approach

Figure 3 shows the entire flowchart of the proposed approach. In order to identify the color bands in resistor image, the main body of resistor and its color bands should be segmented following the resistor being adjusted into a horizontal base, and thus an effective thresholding algorithm is needed. In this study, a thresholding method modified from the Niblack[15,16] and NICK algorithms[17] is evaluated and adopted, which will be used in Stage 1 and Stage 3. Before the color band extraction and color identification, the main resistor's body should be located as close as to cover all color bands (Stage 2). In the stage of color identification (Stage 4), in order to avoid color classifier being confused and overcome the similarity problem with different colors, one database for background color and two databases used individually for 4-band and 5-band resistor are considered in our design. Since the resistor has been aligned horizontally, refer to Table 1, the sequence of color codes may be in order or reversed. Thus the sequence analysis of color codes is needed (Stage 5). In what follows, the details of our algorithms will be presented according to the flowchart in Fig. 3.

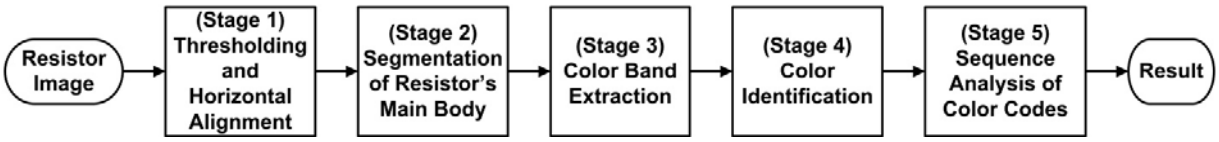

Fig. 3 Flowchart of our image processing algorithms.

3.1 Thresholding and Horizontal Alignment for a Resistor

Several thresholding algorithms have been reported.[15-23] The thresholding methods including local,[15-17] global,[18] dynamic,[19-21] or mixed[22,23] ones have been widely developed for image binarization. The key principle of Niblack's algorithm[15] is to compute each pixel-wise threshold

by sliding a window over the entire image. Each threshold is determined by the local mean and standard deviation of all gray values in the window. Such a local adaptive thresholding scheme is suitable for the resistor image thresholding due to the three-dimensional surface for a color-band resistor. Because the parameters used in Niblack-like thresholding methods will depend on the applications, based on the algorithms from Niblack[15,16] and NICK,[17] a modified thresholding formula, is presented as follows to get better results for the segmentation of resistor's body and its color bands. The color resistor image will be converted into a gray image, and a sliding window is used for thresholding.

$$T = m + \sqrt{\frac{j}{n}\sum_{\forall i} g_i^2} \tag{4}$$

Where m is the local sample mean, g_i denotes the gray value of the i-th pixel, n is the total number of pixels in the window, and j is the newly defined factor which includes the original Niblack's deviation factor k and can be adjusted to get a better result not only for thresholding but also for noise suppression compared to the original works.

Equation (4) will be used in the segmentation of not only resistor's body for detecting resistor orientation (Stage 1) but also color bands for color training and identification (Stage 3). At Stage 1, the factor j can be set at a wide range [0.00008, 0.0036] or even more, whereas $j = 3.6 \times 10^{-3}$ is used at Stage 3 according to the investigation of signal-to-noise ratio (SNR) presented in Appendix. A 4-band (brown-red-orange-gold) resistor and its binarized result obtained by our scheme with $j = 3.6 \times 10^{-3}$ are shown in Fig. 4(a) and 4(b), respectively. Note here that the binarized result is composed of the resistor's body and two wire terminals.

To find the resistor region, in our approach a median filtering is applied first and then the convex hull is used to confine the resistor region as shown in Fig. 4(c). However, the obtained resistor binary image may be divided into more than one region due to the color band effect. For

example, given a 5-band (brown-silver-black-gold-blue) resistor in Fig. 4(e), there are two regions displayed in Fig. 4(g) after the convex hull processing on the binary image shown in Fig. 4(f). Note here that, in this study the principal orientation of resistor is dominated by the largest region from the convex hull result.

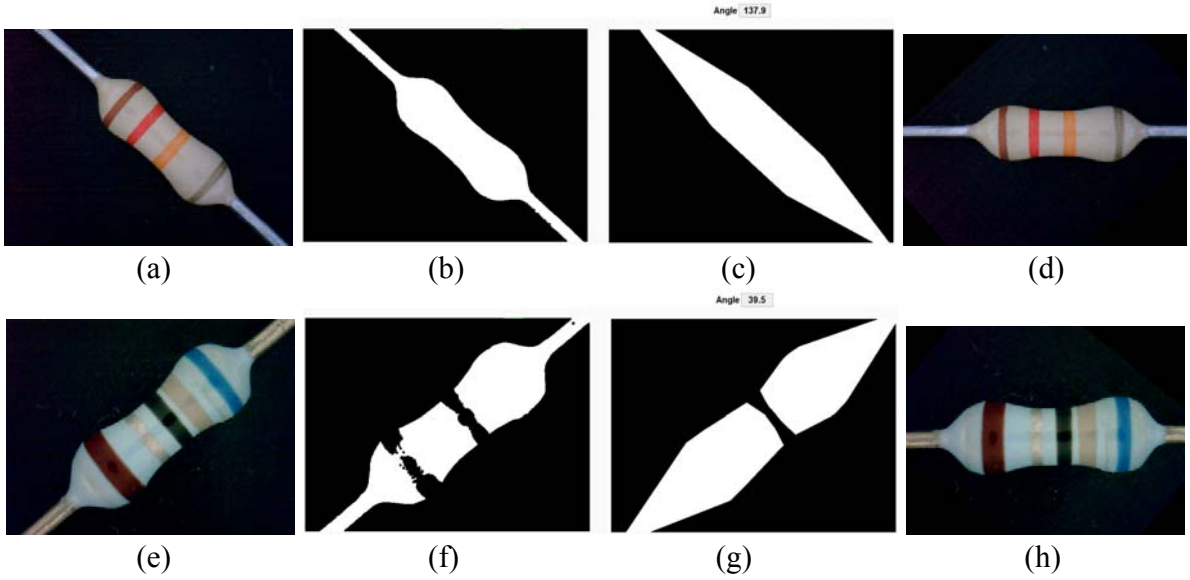

Fig. 4 Illustrations of resistor thresholding and horizontal adjustment. (a) Original image of 4-band (brown-red-orange-gold) resistor; (b) its binarization result; (c) convex hull for orientation detection; and (d) horizontal aligment. (e) Another 5-band (brown-silver-black-gold-blue) resistor image; (f) its binarization result; (g) convex hull for orientation detection; and (h) horizontal aligment.

Once the resistor region is obtained as exemplified in Fig. 4(c) or Fig. 4(g), the principal orientation of the resistor (θ_{rad}) can be readily computed via a moment based method as expressed in Eq. (5). The θ_{rad} is defined to be the line that passes through the region center of mass (centroid) about which the region has the lowest moment of inertia. Here the moment of inertia gives a representation of the pixel distribution in a region with respect to the centroid. Let *A* be the area of the considered region, then the θ_{rad} may be expressed by

$$\theta_{rad} = \frac{1}{2}\tan^{-1}\left(\frac{2M_{xy}}{M_{yy} - M_{xx}}\right) \tag{5}$$

Where $M_{xy} = \sum_{\forall i} x_i y_i - \frac{\sum_{\forall i} x_i \sum_{\forall i} y_i}{A}$, $M_{xx} = \sum_{\forall i} x_i^2 - \frac{(\sum_{\forall i} x_i)^2}{A}$, and $M_{yy} = \sum_{\forall i} y_i^2 - \frac{(\sum_{\forall i} y_i)^2}{A}$. Because the degree unit is adopted in our system as mentioned in Sec. 2, the found orientation θ_{rad} (with radian unit) will be converted to θ_{deg} (with degree unit, i.e., the θ_{dro} as defined before) for the horizontal adjustment of resistor's body. According to this scheme, the resistors can be aligned horizontally as shown in Fig. 4(d) and 4(h) for the current illustrations.

3.2 Segmentation of Resistor's Main Body

To facilitate the extraction of the color bands, the resistor's main body should be confined by removing the unnecessary information such as the outside of resistor surface and the wire terminals. Consider the horizontally aligned image shown in Fig. 4(d) having *W*×*H* pixels for illustration, the first step is to make a rectangle with 80-pixel height centering at the horizontal line and retain the *W*×80 pixels rectangular image as shown in Fig. 5(a). Since the small particles may appear on the black pad and the wire terminals are not involved for color band analysis, they should be further removed. In our scheme, the color image in Fig. 5(a) is converted into a gray image, then an erosion process with 3×3 structure element is applied on the gray image several times, e.g., 20, for obtaining a clean background image as shown in Fig. 5(b) for further processing. By finding the intersection points between consecutive pixels on the top and bottom borders, we can find the left-most and right-most *x*-border point for the top border line, denoted by $(x_{left}^{top}, x_{right}^{top})$ = (205, 499); and the bottom border line, denoted by $(x_{left}^{bottom}, x_{right}^{bottom})$ = (210, 496), respectively. By taking the maximum of x_{left}^{top} and x_{left}^{bottom} for the left border ($x_{left} = 210$) as well as the minimum of x_{right}^{top} and x_{right}^{bottom} for the right border ($x_{right} = 496$), the rectangular image shown in Fig. 5(a) can be further confined as shown in Fig. 5(c), which is the

obtained resistor's main body and will be used for further color band extraction. Note here that the width of segmented resistor body is denoted by $W_{resistor} = x_{right} - x_{left} + 1$ =287.

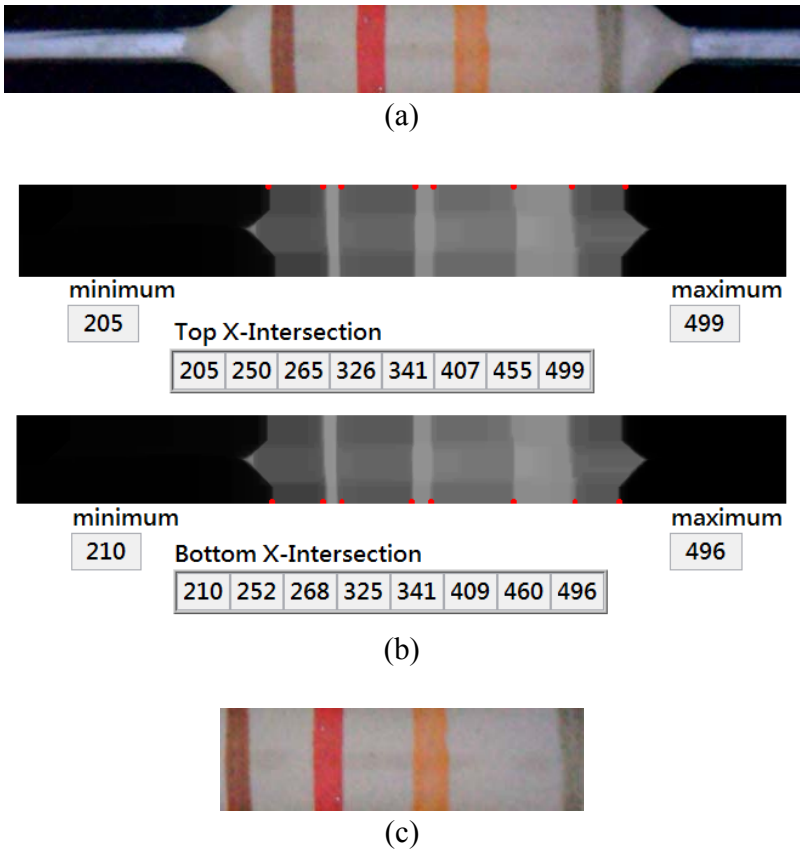

Fig. 5 Illustration of segmenting the resistor's main body. (a) The *W*×80 pixels rectangular image found first. (b) The image having a clean background, where the intersection points on the top and bottom borders are marked in RED color. (c) The obtained resistor's main body.

3.3 Color Band Extraction

Fundamentally, the colored surface of a resistor consists of one colored body and several colored bands. The color of colored body is treated here as the background color in order to form a background image for image subtracting. Since the background color (*BC*) is always the majority one as Fig. 5(c) shows, without use of a high computation cost algorithm[1,24] the extraction of color bands can be initially performed by subtracting the *BC* from the original color image data.

By analyzing the RGB histograms for the resistor's main body image, the $BC = (R_{bc}, G_{bc}, B_{bc})$ can be obtained from their peaks. Figure 6 shows the histograms of Fig. 5(c), where the found BC is (163, 157, 156). In usual, the BC of 4-band resistor (BC_4) and that of 5-band resistor (BC_5) is rather different, e.g., the BC towards "gray" color as shown in Fig. 7(a) in the current 4-band example, whereas the 5-band resistor image in Fig. 4(h) towards "light blue" color. Therefore, except for the number of color bands, the BC information is also adopted in our system for checking whether the considered resistor belongs to 4-band or 5-band.

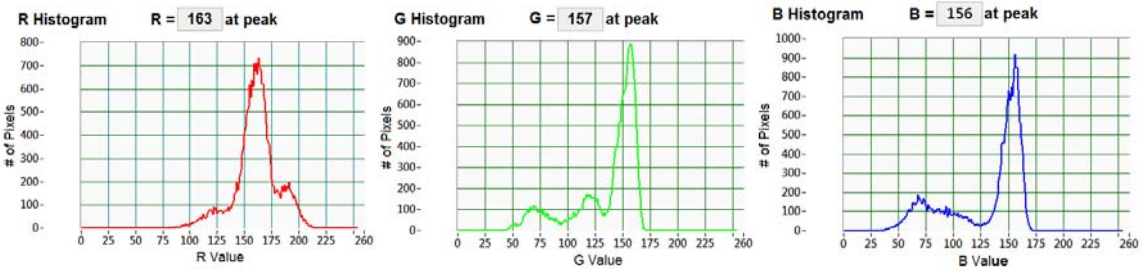

Fig. 6 The RGB histograms and their peaks for the image given in Fig. 5(c). In this case, the found background color is (163, 157, 156).

(a) (b) (c)

Fig. 7 (a) The background image generated by the found background color (163, 157, 156). (b) The image obtained by absolutely subtracting the background information in (a) from the original image in Fig. 5(c). The binarized result by our thresholding scheme with $j = 3.6\times10^{-3}$.

After obtaining the background color BC, the background image can be generated as shown in Fig. 7(a). By absolutely subtracting the background information from the original image in Fig. 5(c), the differencing image can be obtained as shown in Fig. 7(b). After converting this color image into the gray one, the binarized image can be obtained as displayed in Fig. 7(c) by our thresholding scheme with $j = 3.6\times10^{-3}$. This result can be readily used for the following

extraction of color bands. Note here that the determination of j used in our thresholding algorithm is based on this stage and described in Appendix.

By inspecting the binarized image in Fig. 7(c), it is obvious that the color bands appear within the "white" regions, where the "black" regions are regarded as the background in this case. Therefore, with the connected-component processing we can locate n color-band-like regions, namely $CBL_i, i = 1, 2, \ldots, n$, and let (xc_i, yc_i) and h_i denote its corresponding centroid and height. In addition, let the *CBL*'s width be confined to be 20 pixels centering at *xc*. Thus the rectangular region for a CBL_i can be located as $20 \times h_i$ pixels. Since the height of the image in Fig. 5(c) is already known as 80 pixels defined in Sec. 3.2, the *CBL* region having 80-pixel height will be remained as the final color band (*CB*). It is reasonable that the number of *CB*s can be determined based on this requirement. However, a wanted CBL_i could be not counted in due to its $h_i < 80$. Fortunately, the BC_4 and BC_5 information mentioned previsously can be involved to overcome this problem. Two rules as follows are therefore used for determining the number of color bands.

(1) If the number of *CB*s is equal to 5, then it is a 5-band resistor. Otherwise go to Rule 2.

(2) If the background color tends towards BC_4 (BC_5), it is a 4-band (5-band) resistor.

In the current illustration, except for the background color given in Fig. 7(a), we have four *CB*s having 80-pixel height and their *xc* information are 14, 84, 165, and 277, respectively. After applying such a mechanism, it is satisfied to Rule 2 in which the background color towards BC_4, and the four *CB* images are thus obtained as shown in Fig. 8.

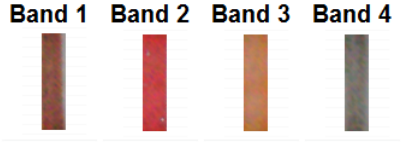

Fig. 8 Four extracted color band images with 20×80 pixels for the image given in Fig. 5(c).

3.4 Color Identification

After determining the number of color bands and extracting the color bands from a resistor image, the small-size image of each color band (i.e., the *CB* image) will be collected into a data set for further training and identification according to it belongs to 4-band or 5-band resistor. Due to the color variation on the resistor surface, to identify accurately the color is not an easy task. The strip colors used in color bands are not precisely standard. In addition, several band's colors are quite similar. For instance, the colors among gray, white, silver are similar; and those among orange, red, brown are similar too. In addition, some band's colors with the same color name may also be different between 4-band and 5-band resistor. For example, silver band color in 4-band resistor is somewhat different to that in 5-band resistor as displayed respectively in Fig. 9(a) and 9(b); and silver band color in 5-band shown in Fig. 9(b) is similar to gold ones in 4-band as shown in Fig. 9(c). Therefore, in this study two databases (DB_4 and DB_5) are built individually for 4-band and 5-band color identification as some of *CB* images listed in Fig. 10. In addition, the third database (DB_{BC}) is also built for checking if the background color on a resistor body belongs to a 4-band or 5-band one. Note here that refer to the mapping table in Table. 1, there are 12 categories in DB_4 and DB_5 for mapping the color band into color code, multiplier, and tolerance; whereas the DB_{BC} has only 2 color categories for distinguishing 4-band and 5-band resistor.

Without use of complex method such as fuzzy c-means clustering,[25] for training the three databases, DB_{BC}, DB_4 and DB_5, a mechanism with *K*-Nearest Neighbor (*K*-NN) classifier is presented in Fig. 11. In this study, the NI (National Instruments) color classification interface[26] is adopted to train and classify the extracted colors. Since the HSL (hue, saturation, lightness) color space has been applied effectively in many fields, e.g., color analysis on yarn-dyed fabric,[27] the

HSL instead of RGB is used here for color classification, where the conversion from RGB to HSL[27-29] may be realized as follows. Let $V_1 = 2R - G - B$, $V_2 = \sqrt{3}(G - B)$, and a degree φ related to (V_1, V_2) be defined as

$$\varphi = \begin{cases} \tan^{-1}(V_2/V_1), & \text{if } V_1 \neq 0, \\ \pi/2, & \text{else if } V_1 = 0 \text{ and } V_2 > 0, \\ -\pi/2, & \text{else if } V_1 = 0 \text{ and } V_2 < 0, \\ 0, & \text{otherwise.} \end{cases} \tag{6}$$

Then the H, S, and L are

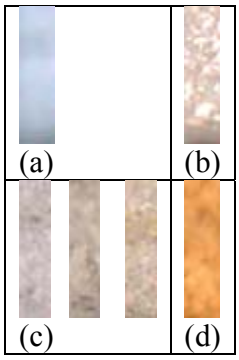

Fig. 9 Illustrations of color inconsistency of silver and gold color in 4-band and 5-band resistor. Silver band colors in (a) 4-band and (b) 5-band resistor. Gold band colors in (c) 4-band and (d) 5-band resistor. Note here that silver band color in 5-band resistor is similar to gold band color in 4-band resistor.

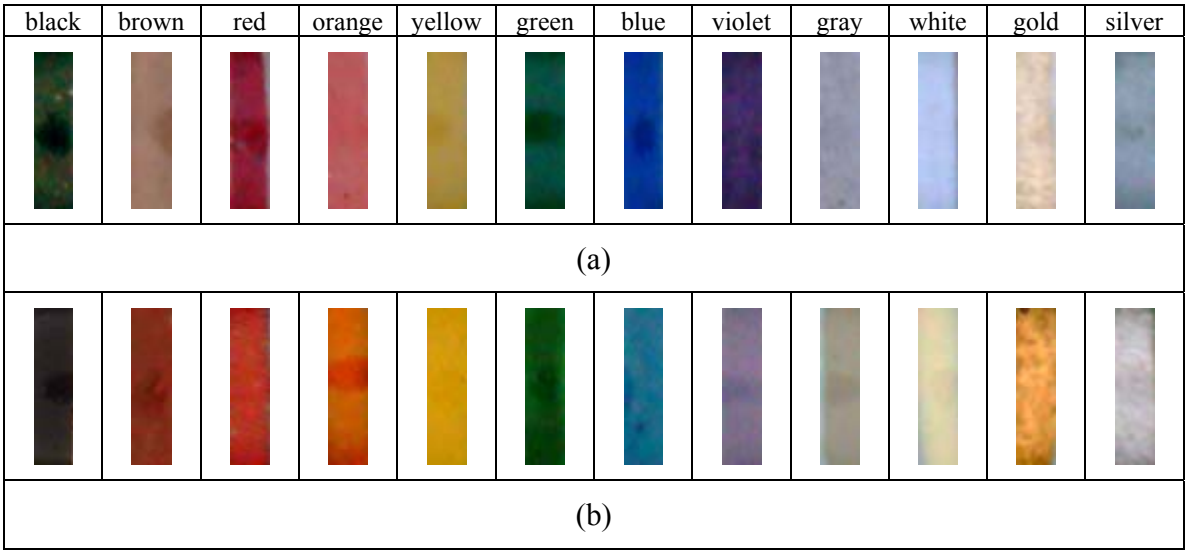

Fig. 10 Some color band images with 20×80 pixels extracted from (a) 4-band and (b) 5-band resistors.

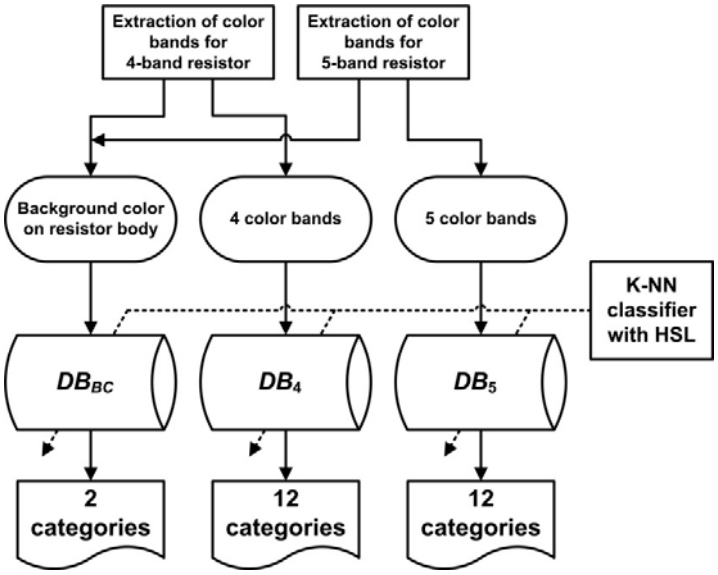

Fig. 11 Color training/identification mechanism for the three databses in our system.

$$H = \begin{cases} 256\varphi/2\pi, & \text{if } V_1 \geq 0,\ V_2 \geq 0, \\ 256(\pi + \varphi)/\pi, & \text{else if } V_1 > 0, \\ 256(2\pi + \varphi)/\pi, & \text{otherwise.} \end{cases} \tag{7}$$

$$S = 255\left(1 - 3\min(R, G, B)/(R + G + B)\right) \tag{8}$$

$$L = 0.299R + 0.587G + 0.114B \tag{9}$$

By the *K*-NN classifier, a color is classified into a class based on a voting mechanism. The classifier finds *K* nearest samples from all the classes. The unknown color sample is assigned to the class with the majority of the votes in the *K* nearest samples. In our experiments, *K*=3 is sufficient for training and classifying colors. During the database is being trained, the extracted band's color will be treated as a sample test and computed by the *K*-NN algorithm. If it matches with one color category, the current *CB* (or *BC*) image will be added into this category. It means that one color category in the database may include several trained *CB* (or *BC*) images. For example, for *CB*'s color training, some *CB* samples are trained as 4-band "brown" color category as shown in Fig. 12(a), and those trained as 5-band "silver" color category in Fig. 12(b). In addition, for background color training, some *BC* samples are trained as 4-band "background"

color category as shown in Fig. 12(c), and those trained as 5-band "background" color category in Fig. 12(d). Note again that DB_4, DB_5, and DB_{BC}, maintain 12, 12, and 2 color categories, respectively in our system as depicted in Fig. 11, and they will be used individually depending on which path is going on while the color identification is performed. For example, if the one *CB* image comes from a 4-band resistor, it will be matched with the *CB* samples in DB_4, the color category containing the most matched *CB* sample is just we want. Based on such an identification mechanism, the found colors are "brown", "red", "orange", and "gold" for the four *CB*s shown in Fig. 8. They are coded as "1-2-3-10" according to the reading sequence from left to right and the mapping table in Table. 1. As a result, the 4-band resistor is read as $R_4 = 12 \times 10^3 \pm 5\%\ \Omega$ based on Eq. (1).

3.5 Sequence Analysis of Color Codes

For reading a resistor value, the reading sequence of color codes is from left to right as formed in Table 1. That is, the tolerance band should be at the right-most side. Since the resistor was put on the pad at random orientation, the tolerance band may be located at the left-most side or right-most side in the resistor image after horizontally alignment process. Therefore, it is necessary for analyzing the sequence of color bands. In rule of the considered resistor (refer to Table 1), for 4-band resistors the tolerance band is only represented by gold or silver color, whereas for 5-band resistors it may also be represented by other colors, e.g., brown, red, green, blue, violet, and gray color; as well as the multiplier may also be represented by gold or silver color. In addition, it is found that the distance between multiplier band and tolerance band is usually greater than that between any other two adjacent color bands, in particular, for 5-band resistors. Based on these observations, the sequence of color codes should be flipped over if any one of the following rules is satisfied.

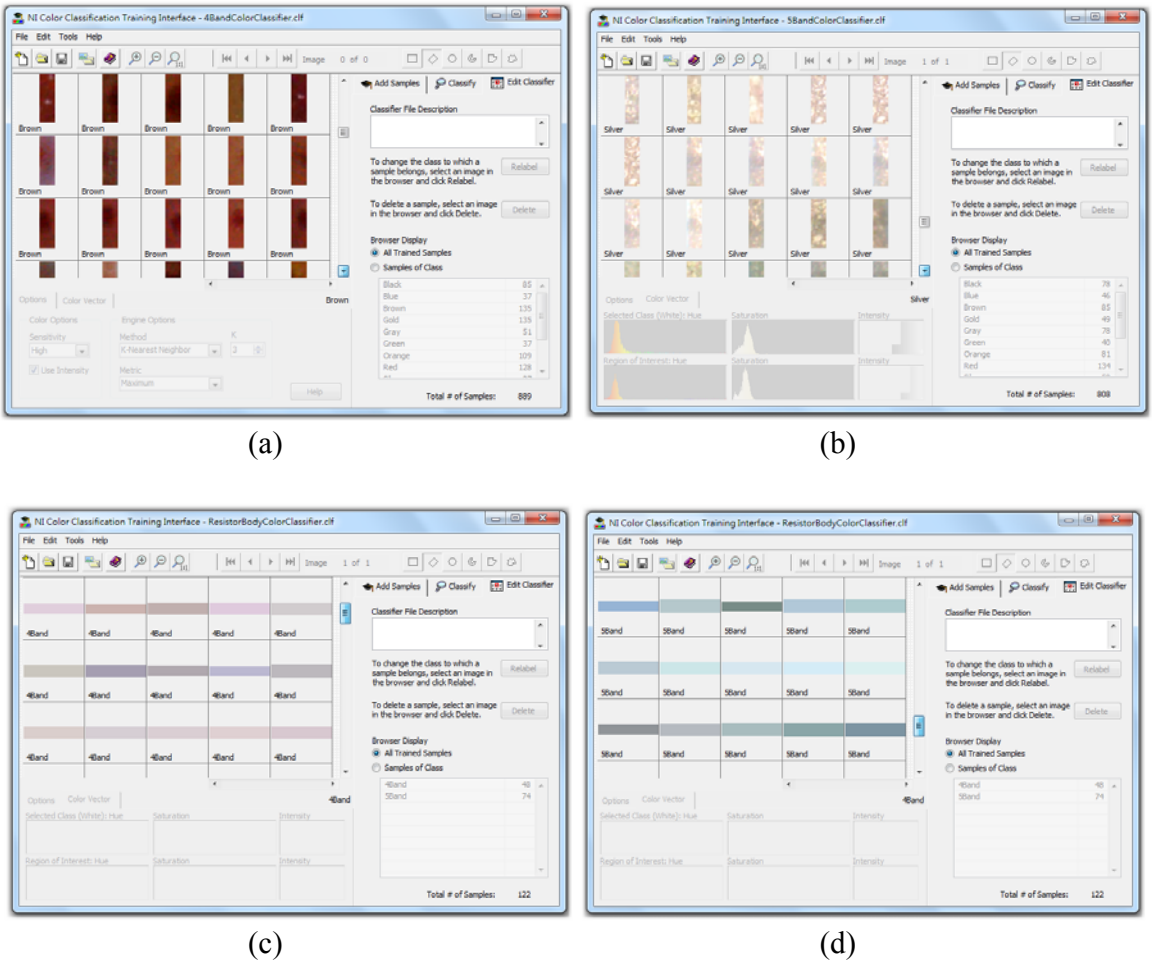

Fig. 12 NI color classification interface adopted in our system. (a) Some color band samples are trained as 4-band "brown" color category, and (b) those trained as 5-band "silver" color category. (c) Some background color samples are trained as 4-band "background" color category, and (d) those trained as 5-band "background" color category.

(1) The left-most or the second-left color band is recognized as gold or silver color, or

(2) the distance between the left-most two color bands (d_{1L-2L}) is greater than that between the right-most two color bands (d_{1R-2R}).

With the same resistor as given in Fig. 4(a) but put in different orientation, the recognized result is reported in Fig. 13(a). It can be found that the left-most color band is of gold. Thus it is flipped over according to Rule 1 and the computed resistor value is correct, i.e., $R_4 = 12 \times 10^3 \pm 5\%\ \Omega$. In addition, for the 5-band resistor image given in Fig. 4(e), the result reported in Fig. 13(b) is

also correct, i.e., $R_5 = 680 \times 10^{-2} \pm 1\%\ \Omega$, where the second-left color band is of silver. From both results given in Fig. 13, they are also satisfied to the Rule 2.

(a)

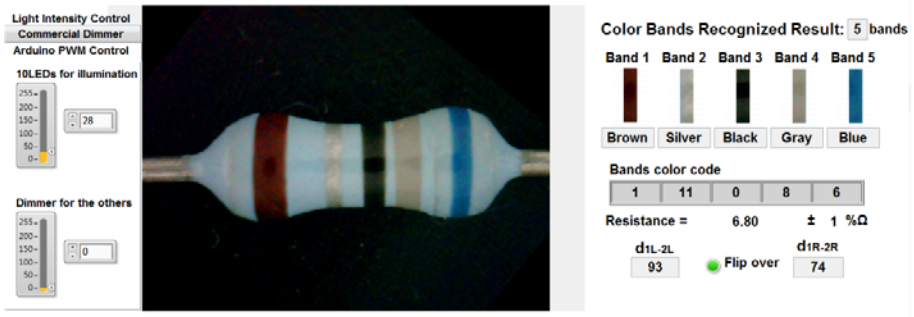

(b)

Fig. 13 Illustration of flipping over the sequence of color codes for the case of (a) 4-band and (b) 5-band resistor.

4 Results and Discussions

The system implementation for the proposed approach is presented in Sec. 4.1. In addition, with the developed algorithms for reading resistor, the performances of several diffuse light sources including the commercial products and the self-made cost-effective ones are compared in terms of SNR and recognition results. Because the dome of light source is replaceable, the microscope calibration is needed for system setup as illustrated in Sec. 4.2. Finally, the performances of the entire system are reported in Sec. 4.3, where a suggestion for the proper range of luminous intensity is derived based on experiments.

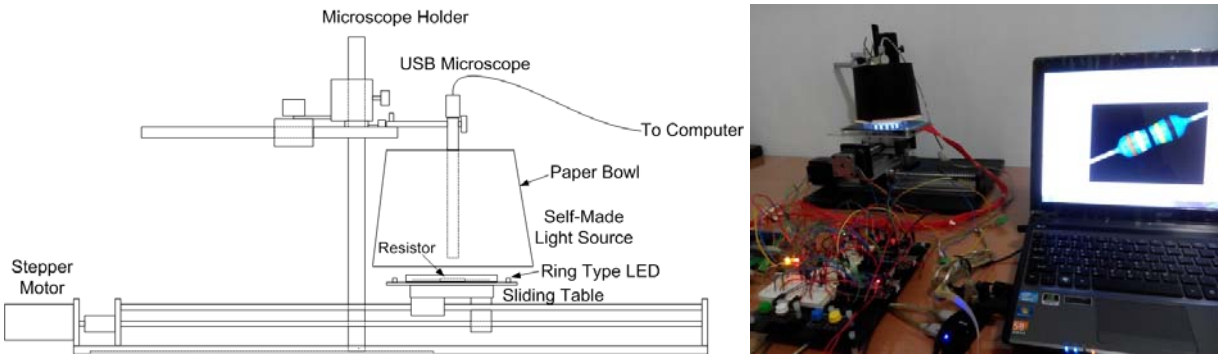

(a) (b)

Fig. 14 (a) Mechanism for the light source setup, where the sliding table controlled by a stepper motor is used to carry the resistor for reading. (b) System implementation.

4.1 System Implementation and Comparison of Light Sources

In accordance with the block diagram of the developed system in Fig. 1, the mechanism for the light source is depicted in Fig. 14(a), where the sliding table controlled by a stepper motor is used to carry the resistor for reading. Our system implementation is shown in Fig. 14(b). To investigate the effects of specular reflection and halo on resistor surface which will affect the recognition of resistor color bands, several types of commercial light sources and self-made ones as listed in Table 2 and Fig. 15 are used for experiments and comparisons. They include one room light without control, four commercial lights, and five self-made lights. For the cost-effective self-made light sources, their light reflections are taken from a replaceable paper bowl, cup or box inside pasted with white paper to reduce specular reflection and halo effect on the resistor surface. One 4-band resistor (orange-black-brown-gold) and one 5-band resistor (green-white-black-red-brown) are used for evaluations. In these evaluations, the recognition results are correct for all the cost-effective self-made diffuse light sources (Type 6-10, note here that their SNRs are relative high), whereas they are incorrect for the Type 4 commercial product. Compare among the commercial products, the result from Type 5 is the best one since the dome can

support a better light reflection. By further observing our cost-effective diffuse light sources (Type 6-10) as shown in Fig. 15, it is reasonable that they can also obtain a good result since the structure of paper bowl, cup or box inside pasted with white paper is similar to that of dome used in the Type 5 commercial product. Accordingly, the design of very cheap diffuse light sources which can reduce the effects of specular reflection and halo on resistor surface and are helpful for reading resistor via computer vision is confirmed.

4.2 Calibration of Microscope

Before applying the presented algorithms for resistor recognition, the microscope in the system should be calibrated for each setup since the system is possibly moved more or less during experiments, e.g., changing the paper dome. The calibration process illustrated in Fig. 16 is described as follows. Figure 16(a) shows that a rubber band crossing LED 0 and LED 12 is used to mark the zero degree and regarded as the horizontal base. The microscope will acquire the rubber band image as shown in Fig. 16(b), after the thresholding and convex hull processing the binarized images can be obtained as displayed in Fig. 16(c) and 16(d), respectively. By adjusting (e.g., rotating) the microscope indicated in Fig. 16(a), the rubber band binary image shown in Fig. 16(d) will also be changed. In this way, the angle of rubber band to the horizontal base θ_{dro} and thus $\hat{I}$ can be obtained immediately. According to the algorithms presented in Sec. 3.1 and Eq. (3), the automatically turned-on LEDs represented by $S_{LED-on}(\hat{I})$ can be easily observed. By observing the LEDs and adjusting microscope, the microscope can be easily calibrated as Fig. 16(d) shows and fixed for the subsequent experiments.

Table 2 Several types of light sources used to investigate the effects of specular reflection and halo in resistor recognition. They are displayed respectively in Fig. 15. The 4-band resistor with orange-black-brown-gold color bands and the 5-band resistor with green-white-black-red-brown color ones are used for evaluations. Here "∞" represents that no noisy pixels found in the case, and "NA" represents that the segmentation of color bands fails due to the severe specular reflection.

Light source	Description	Recognition result for a 4-band resistor		Recognition result for a 5-band resistor	
		SNR	Correct	SNR	Correct
Type 1	Room light without control	19.5	v	5.3	x
Type 2	Ring type low angle (60°) light (*commercial product*)	49.6	v	391.2	v
Type 3	Ring type low angle indirect light with emitting surface of 127mm (Φ) (*commercial product*)	17.9	v	172.9	v
Type 4	Coaxial light of 50mm×50mm (*commercial product*)	43.4	x	NA	x
Type 5	Dome diffuse light of 108mm(Φ)×66mm(H) (*commercial product*)	297.9	v	2884	v
Type 6	*Self-made* diffuse light with paper bowl of 103mm(Φ) ×67mm(H)	5923	v	6116	v
Type 7	*Self-made* diffuse light with paper bowl of 130mm(Φ) ×65mm(H)	1195	v	∞	v
Type 8	*Self-made* diffuse light with paper bowl of 133mm(Φ) ×99mm(H)	∞	v	∞	v
Type 9	*Self-made* diffuse light with paper box of 165mm(L) ×155mm(W) ×110mm(H)	∞	v	∞	v
Type 10	*Self-made* diffuse light with paper cup of 97mm(Φ) ×125mm(H)	∞	v	1511.8	v

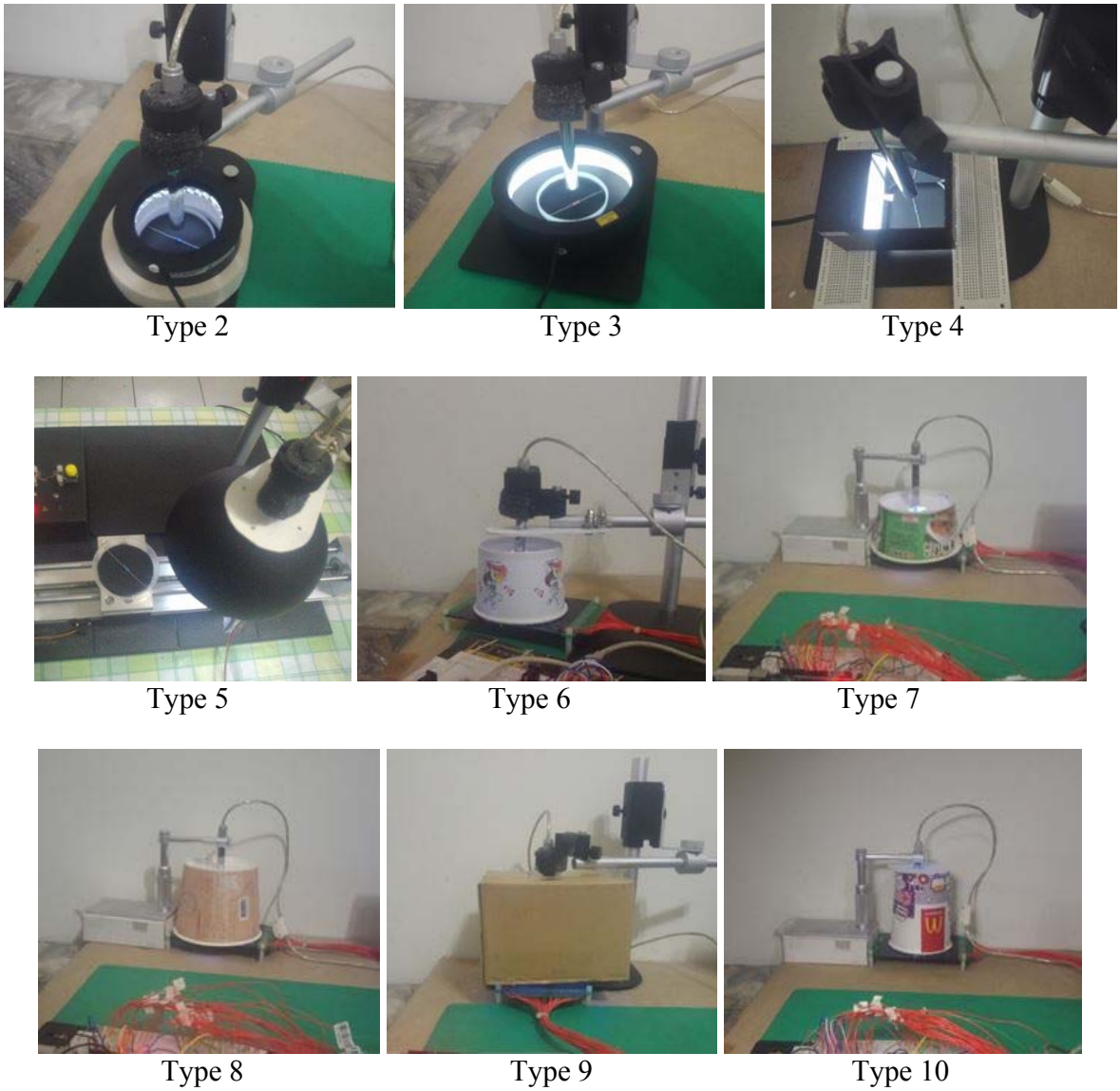

Fig. 15 Four commercial light sources (Type 2-5), and five cost-effective self-made light sources (Type 6-10). Refer to Table 2 for their descriptions.

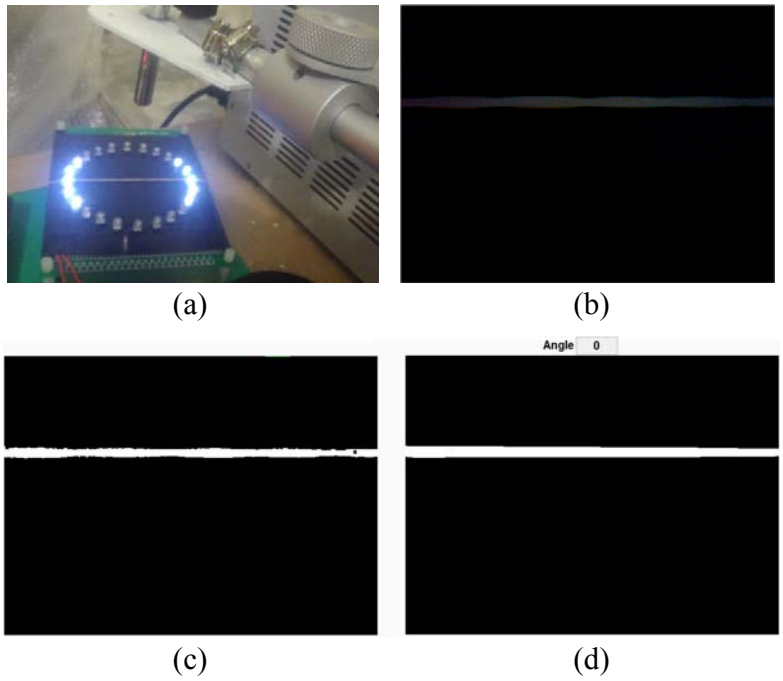

Fig. 16 Calibration of microscope. (a) A rubber band crossing LED 0 and LED 12 is used to mark the zero degree for microscope calibration. (b) The acquired rubber band image. (c) The binarized image by our thresholding scheme. (d) Perform the convex hull processing to the binary image and adjust the microscope to zero degree of rubber band angle for alignment.

4.3 Results by Our Algorithms

In our experiments, the cost-effective self-made light source has a better effect of reducing the specular reflection and halo phenomenon on resistor surface and a better recognition result compared to the commercial light sources. In order to further verify the proposed computer vision approach with our self-made light sources, the algorithms are implemented in LabVIEW combining with the MATLAB codes to acquire 4-band and 5-band resistor images for analysis. The resistor is put on a black pad at random orientation. Each 4-band or 5-band group includes several resistors comprising 12 colors as listed in Table 1. Since the controllable luminous intensity (LI) will affect the quality of acquired resistor image for processing, an appropriate LI should be determined. It can be investigated by analyzing the *CB*'s SNR and recognition result

with respective to the given LI parameter. In this experiment, given an intensity of light source we take the mean of image intensity as the LI value. In usual, to differentiate the color among (brown, red, orange) and that among (white, gray, silver) is somewhat difficult. Therefore, we take a brown-red-orange-gold resistor image and a blue-gray-black-silver-brown resistor image for the LI investigation and their results are reported respectively in Table 3 and Table 4. Based on these investigations, the LI value ranged from 25 to 43 is suggested in our system.

The performances of our system are evaluated by 200 4-band resistors (10 types, 20 resistors/type) as well as 200 5-band resistors (10 types, 20 resistors/type), and reported respectively in Table 5 and Table 6 with the failed number in terms of horizontal alignment, color band extraction, color identification, and color code sequence flip over checking. These resistors are with the specification of 1/4 watt and comprise all 12 colors as listed in Table 1. Figures 17 and 18 demonstrate some recognition results of 4-band and 5-band resistors listed in Table 5 and 6, respectively. For the color code sequence flip over checking, our system performs very well. One error appearing in horizontal adjustment is due to the over bending of the resistor metal rod that could result in a mistake of detecting the resistor orientation. Several errors appearing in others are due to the failed color identification among (white, silver, gray) and that among (brown, red, orange) colors. Based on the present experiments, the recognition rate of 93% for 4-band and 88% for 5-band were achieved. As a result, the resistor band's color can be extracted properly for color training and identification by means of using a well-controlled steady light environment and HSL color space. With adequate training and classifying, the performance of color band identification can be improved continuously. So far the capability of identifying the necessary colors used in 4-band and 5-band resistors has been confirmed in this study. Since the manufactures did not always follow a standard of colors, the current color

training databases do not cover all the colors that manufactures used. Fortunately, based on the color classifiers for resistor recognition we have made, the user can still add colors in and modify the present databases. With more training, it is expectable that the more reliable recognition for resistor image can be achieved indeed.

Table 3 LI analysis corresponding to SNR and recognition results by a brown-red-orange-gold resistor image.

LI	SNR	Correct	Error description
17.0	93.2	x	gold recognized as black orange recognized as red
19.2	119.6	x	gold recognized as black orange recognized as brown
22.3	266.7	v	
25.4	122.1	v	
27.5	165.7	v	
29.8	189.7	v	
32.1	337.0	v	
34.2	242.0	v	
37.1	275.6	v	
39.6	216.6	v	
43.1	311.7	v	
45.2	3.5	x	incorrect segmentation gold recognized as silver noise recognized as color band
47.0	3.4	x	incorrect segmentation gold recognized as silver noise recognized as color band

Table 4 LI analysis corresponding to SNR and recognition results by a blue-gray-black-silver-brown resistor image.

LI	SNR	Correct	Error description
16.8	34.7	x	silver recognized as gray
19.3	47.4	x	silver recognized as gray
22.2	74.9	v	
25.9	50.5	v	
27.1	106.5	v	
31.9	66.7	v	
34.1	132.5	v	
35.6	96.2	v	
38.8	69.1	v	
42.5	152.1	v	
43.9	109.4	v	
46.6	271.8	x	gray recognized as silver
49.0	105.7	x	silver recognized as white gray recognized as silver

Table 5 Results by 10 types of 4-band resistors. Each type contains 20 resistors. The errors result from horizontal alignment, color band extraction, color identification, and color code sequence flip over checking are reported by failed numbers. The total number of failed recognition is 14, and thus the recognition rate is 93%.

Resistor type	Failed numbers				
	Horizontal alignment	Color band extraction	Color identification	Flip over checking	Subtotal
Brown-Red-Orange-Gold	0	1	2	0	3
Brown-Black-Orange-Gold	0	1	0	0	1
Green-Blue-Red-Gold	0	0	0	0	0
Gray-Red-Black-Gold	0	0	1	0	1
Red-Violet-Yellow-Gold	0	0	0	0	0
Green-Brown-Green-Silver	0	1	2	0	3
Yellow-Violet-Brown-Gold	0	0	1	0	1
Blue-Gray-Red-Gold	0	0	2	0	2
Orange-White-Yellow-Gold	0	1	2	0	3
Orange-White-Red-Gold	0	0	0	0	0
Total	0	4	10	0	14

Table 6 Results by 10 types of 5-band resistors. Each type contains 20 resistors. The errors result from horizontal alignment, color band extraction, color identification, and color code sequence flip over checking are reported by failed numbers. The total number of failed recognition is 24, and thus the recognition rate is 88%.

Resistor type	Failed numbers				
	Horizontal alignment	Color band extraction	Color identification	Flip over checking	Subtotal
Blue-Gray-Black-Silver-Brown	0	2	2	0	4
White-Violet-Blue-Orange-Brown	1	0	0	0	1
Yellow-Violet-Black-Silver-Brown	0	0	1	0	1
Brown-Gray-Black-Gold-Brown	0	1	2	0	3
Brown-Green-Black-Gold-Brown	0	0	1	0	1
Violet-Green-Black-Silver-Brown	0	2	2	0	4
White-Brown-Black-Silver-Brown	0	1	2	0	3
Red-Green-Black-Orange-Brown	0	1	2	0	3
Gray-Red-Black-Orange-Brown	0	2	1	0	3
Green-Brown-Black-Yellow-Brown	0	0	1	0	1
Total	1	9	14	0	24

(a)

(b)

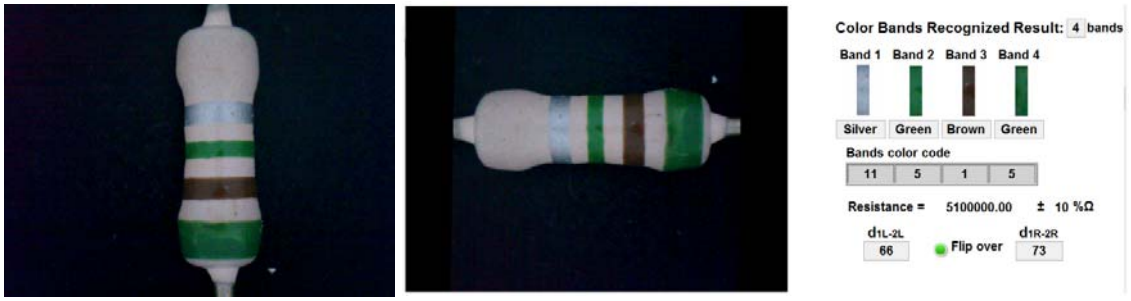

(c)

(d)

Fig. 17 Some recognition results of 4-band resistors from the set listed in Table 5**.**

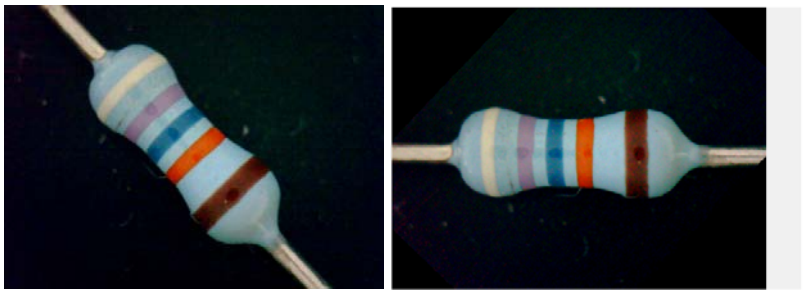

(a)

(b)

(c)

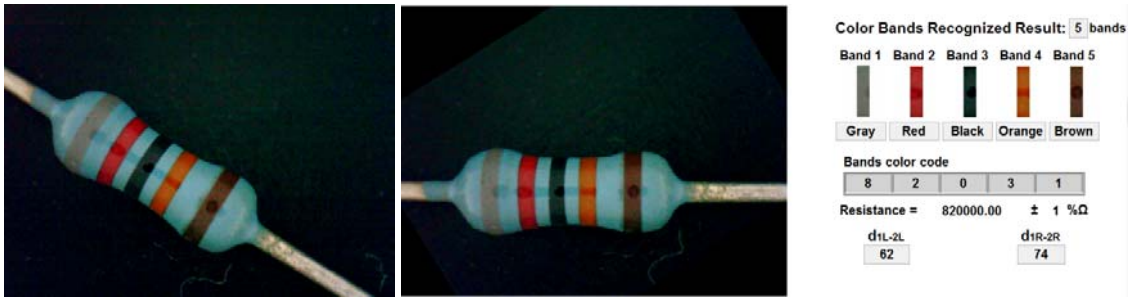

(d)

Fig. 18 Some recognition results of 5-band resistors from the set listed in Table 6**.**

5 Conclusions

On the study of reading color-band resistor via computer vision, due to the resistor's specular reflective surface it will face with a severe non-uniform luminous intensity on image yielding a higher error rate in recognition without a well-controlled light source. A computer vision system including mainly a digital microscope embedded in a replaceable diffuse cover, a controllable ring-type LED embedded onto a small pad carrying a resistor, and Arduino microcontrollers connected with PC, has been presented so far. Several replaceable cost-effective diffuse covers made by paper bowl, cup and box inside pasted with white paper has been experimented for reducing specular reflection and halo effects compared with a commercial diffuse dome. The ring-type LED can be flexibly configured to be a full or partial lighting according to the detected resistor orientation, which is useful to further reduce the specular reflection and make the acquired resistor image to be easily processed. For processing a resistor image, the presented algorithms are mainly composed of thresholding and horizontal alignment, segmentation of resistor's main body, color band extraction, color identification, as well as sequence analysis of color codes for finally reading the resistor value. Experimental results on 200 4-band resistors and 200 5-band resistors have confirmed that the proposed system can not only evaluate the cost-effective diffuse light sources but also can automatically read the resistor value. As a future work, it is expected that the proposed system can be applied for recognizing multiple resistors from an image and extended to the other color material recognition. In addition, some related reflectance and color mathematical models are worthy of studying in the future to support the design of computer vision algorithm and cost-effective light sources.

Appendix: Selection of factor *j* used in our thresholding method

According to our approach shown in Fig. 3, the modified thresholding in Eq. (4) may be used in the segmentation of not only resistor's body for detecting resistor orientation (Stage 1) but also color bands for color classification and identification (Stage 3). At Stage 1, according to our experiments the factor j can be set at a wide range [0.00008, 0.0036] or even more due to the adoption of median filtering and convex hull processing. The window size adopted at this stage is the same as the image size, i.e., 640×480 pixels. At Stage 3, the factor j is determined by the investigation of signal-to-noise ratio (SNR) since the correctness of color band extraction is of great importance to the color code conversion. Note here that S and N denote the number of pixels in color bands, and that of pixels in non-color-band region, respectively, for a segmented resistor body (refer to Sec. 3.2). By thresholding a 4-band (brown-red-orange-gold) resistor in Fig. 4(a) with various j values, the relationship between j and SNR can be obtained as Fig. 19 shows. In this plot, $j = 3.6 \times 10^{-3}$ is suggested where the SNR starts at a stable high mark. At Stage 3, the window size is defined by $W_{resistor} \times 95$. Here $W_{resistor}$ is the width of segmented resistor body as denoted in Sec. 3.2. With the suggested j value, our scheme can get a better result compared to that of Niblack[15] and NICK[17] for binarizing a brown-red-orange-gold resistor image as reported in Table 7.

Acknowledgments

This work was supported in part by the Ministry of Science and Technology, Taiwan, Republic of China, under the grant number MOST103-2221-E-155-040.

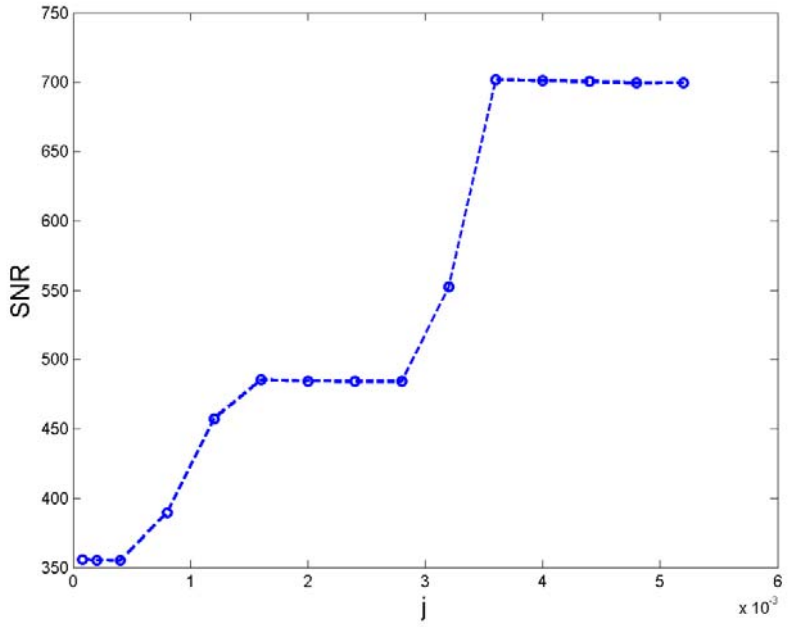

Fig. 19 Relationship between factor j and SNR of the adopted thresholding expression, where $j = 3.6\times10^{-3}$ is suggested and used in our current study.

Table 7 Simple SNR comparison among Niblack[15], NICK[17] and our method (with $j = 3.6\times10^{-3}$) for binarizing a brown-red-orange-gold resistor image.

Methods	S	N	SNR
Niblack[15]	7818	22	355.36
NICK[17]	7811	21	371.95
Our Method	7821	11	701.91

References

1. Y. S. Chen and Y. C. Hsu, "Image segmentation of a color-blindness plate," *Applied Optics* **33**(29), 6818-6822 (1994) [doi: 10.1364/AO.33.006818].
2. Y. S. Chen and Y. C. Hsu, "Computer vision on a colour blindness plate," *Image and Vision Computing* **13**(6), 463-478 (1995) [doi:10.1016/0262-8856(95)94380-I].
3. "Specular vs. diffuse reflection," < http://www.physicsclassroom.com/class/refln/Lesson-1/Specular-vs-Diffuse-Reflection >.
4. K. L. Chan and H. Wang, "Reading resistor values by color image processing," in Automatic Inspection and Novel Instrumentation, T. S. Ho, S. Rao, and L. M. Cheng, Ed., *Proc. SPIE* **3185**, 157-168 (1997) [doi:10.1117/12.284040].
5. Y. Mitani, Y. Sugimura, and Y. Hamamoto, "A method for reading a resistor by image processing techniques," in Knowledge-Based Intelligent Information and Engineering Systems, I. Lovrek, R. J. Howlett, and L. C. Jain, Ed., Part I, *Proc. LNAI* **5177**, 433-439 (2008) [doi: 10.1007/978-3-540-85563-7_56].
6. Y. Mitani and Y. Hamamoto, "A study of color features for reading a resistor," *Proc. SICE Annual Conference*, 2850-2851 (2010).
7. P. R. Claxton and E. K. Y. Kwok, "The use of colour to segment and label images," *Proc. 3rd Alvey Vision Conference*, 295-302 (1987).
8. B. Benchoff, "Reading resistors with OpenCV," < http://hackaday.com/2015/05/14/reading-resistors-with-opencv/ >, 2015
9. "Optical recognition of resistor codes," < http://labrigger.com/blog/2012/03/05/optical-recognition-of-resistor-codes/ >, 2012.
10. Y. S. Chen and J. Y. Wang, "Reading resistor based on image processing," *Proc. of International Conference on Machine Learning and Cybernetics*, 566-571 (2015) [doi: 10.1109/ICMLC.2015.7340616].

11. Y. S. Chen and J. Y. Wang, "Implementation of cost-effective diffuse light source mechanism to reduce specular reflection and halo effects for resistor-image processing," in Applications of Digital Image Processing XXXVIII, A. G. Tescher, Ed., *Proc. SPIE* **9599**, 959928 (2015) [doi:10.1117/12.2187895].
12. "Arduino," < http://www.arduino.cc/ >.
13. K. Szolusha, "Dimming LEDs with pulse-width modulation," < http://www.eetimes.com/document.asp?doc_id=1281013 >, 2013.
14. "Dimming by using pulse width modulation (PWM)," < http://www.sinrace.com.cn/en/knowledge-base/666-dimming-by-using-pulse-width-modulation-pwm.html >.
15. W. Niblack, *An Introduction to Digital Image Processing*, Prentice-Hall International Inc., Englewood Cliffs, New Jersey (1986).
16. S. Farid and F. Ahmed, "Application of Niblack's method on images," *Proc. International Conference on Emerging Technologies*, 280-286 (2009) [doi: 10.1109/ICET.2009.5353159].
17. K. Khurshid, I. Siddiqi, C. Faure, and N. Vincent, "Comparison of Niblack inspired binarization methods for ancient documents," in Document Recognition and Retrieval XVI, K. Berkner and L. Likforman-Sulem, Ed., *Proc. SPIE* **7247**, 72470U (2009) [doi:10.1117/12.805827].
18. N. Otsu, "A threshold selection method from gray-level histograms," *IEEE Transactions on Systems, Man and Cybernetics* **9**(1), 62-66 (1979) [doi: 10.1109/TSMC.1979.4310076].
19. J. Bernsen, "Dynamic thresholding of grey-level images," *Proc. 8th ICPR*, 1251-1255 (1986).
20. J. D. Yang, Y. S. Chen, and W. H. Hsu, "Adaptive thresholding algorithm and its hardware implementation," *Pattern Recognition Letters* **15**(2), 141-150 (1994) [doi:10.1016/0167-8655(94)90043-4].
21. J. Sauvola and M. Pietikainen, "Adaptive document image binarization," *Pattern Recognition* **33**(2), 225-236 (2000) [doi:10.1016/S0031-3203(99)00055-2].
22. A. Z. Arifin and A. Asano, "Image segmentation by histogram thresholding using hierarchical cluster analysis," *Pattern Recognition Letters* **27**(13), 1515-1521 (2006) [doi:10.1016/j.patrec.2006.02.022].

23. X. Zheng and Y. S. Chen, "Document image binarisation based on low-rank modelling," *Electronics Letters* **51**(22), 1784-1786 (2015) [doi: 10.1049/el.2015.2289].
24. H. Y. Huang, Y. S. Chen, and W. H. Hsu, "Color image segmentation using a self-organization map algorithm," *Journal of Electronic Imaging* **11**(2), 136-148 (2002) [doi:10.1117/1.1455007].
25. Y. S. Chen, B. T. Chen, and W. H. Hsu, "Efficient fuzzy c-means clustering for image data," *Journal of Electronic Imaging* **14**(1), 013017 (2005) [doi:10.1117/1.1879012].
26. *NI Vision Concepts Manual*, National Instruments Corporation (2009).
27. R. Pan, W. Gao, and J. Liu, "Color clustering analysis of yarn-dyed fabric in HSL color space," *Proc. Word Congress on Software Engineering*, 273-278 (2009) [doi: 10.1109/WCSE.2009.148].
28. A. Koschan and M. Abidi, *Digital Color Image Processing*, John Wiley & Sons, Inc., Hoboken, New Jersey (2008).
29. M. D. Fairchild, *Color Appearance Models*, 3rd Ed., John Wiley & Sons, Inc., Hoboken, New Jersey (2013).

Yung-Sheng Chen is a professor at the Department of Electrical Engineering, Yuan Ze University. He received BS degree from Chung Yuan Christian University in 1983, and the MS and PhD degrees from National Tsing Hua University, Taiwan, in 1985 and 1989, respectively, all in electrical engineering. He is the author of more than 200 papers and has written four book chapters. His current research interests include computer vision, image processing, and medical imaging. He is a senior member of IEEE.

Jeng-Yau Wang has been working in National Chung-Shan Institute of Science and Technology since 1984. He received his BS degree in Mechanical Engineering from Tamkang University in 1984 and MS degree in Industrial Engineering from Polytechnic University of New York in 1995 (Now is Polytechnic Institute of New York University). He is currently a PhD candidate in Electrical Engineering at Yuan Ze University. His research interests include image processing, computer vision, control, photonics, and optoelectronic systems.

Caption List

Fig. 1 Block diagram of the developed system.

Fig. 2 Light source designed by a controllable 24-LED ring-type structure. In this illuatration, $S_{LED-on}(0) = \{22, 23, 0,1,2,10,11,12,13,14\}$ while the $\theta_{dro} = 0°$.

Fig. 3 Flowchart of our image processing algorithms.

Fig. 4 Illustrations of resistor thresholding and horizontal adjustment. (a) Original image of 4-band (brown-red-orange-gold) resistor; (b) its binarization result; (c) convex hull for orientation detection; and (d) horizontal aligment. (e) Another 5-band (brown-silver-black-gold-blue) resistor image; (f) its binarization result; (g) convex hull for orientation detection; and (h) horizontal aligment.

Fig. 5 Illustration of segmenting the resistor's main body. (a) The W×80 pixels rectangular image found first. (b) The image having a clean background, where the intersection points on the top and bottom borders are marked in RED color. (c) The obtained resistor's main body.

Fig. 6 The RGB histograms and their peaks for the image given in Fig. 5(c). In this case, the found background color is (163, 157, 156).

Fig. 7 (a) The background image generated by the found background color (163, 157, 156). (b) The image obtained by absolutely subtracting the background information in (a) from the original image in Fig. 5(c). The binarized result by our thresholding scheme with $j = 3.6\times10^{-3}$.

Fig. 8 Four extracted color band images with 20×80 pixels for the image given in Fig. 5(c).

Fig. 9 Illustrations of color inconsistency of silver and gold color in 4-band and 5-band resistor. Silver band colors in (a) 4-band and (b) 5-band resistor. Gold band colors in (c) 4-band and (d) 5-band resistor. Note here that silver band color in 5-band resistor is similar to gold band color in 4-band resistor.

Fig. 10 Some color band images with 20×80 pixels extracted from (a) 4-band and (b) 5-band resistors.

Fig. 11 Color training/identification mechanism for the three databses in our system.

Fig. 12 NI color classification interface adopted in our system. (a) Some color band samples are trained as 4-band "brown" color category, and (b) those trained as 5-band "silver" color category. (c) Some background color samples are trained as 4-band "background" color category, and (d) those trained as 5-band "background" color category.

Fig. 13 Illustration of flipping over the sequence of color codes for the case of (a) 4-band and (b) 5-band resistor.

Fig. 14 (a) Mechanism for the light source setup, where the sliding table controlled by a stepper motor is used to carry the resistor for reading. (b) System implementation.

Fig. 15 Four commercial light sources (Type 2-5), and five cost-effective self-made light sources (Type 6-10). Refer to Table 2 for their descriptions.

Fig. 16 Calibration of microscope. (a) A rubber band crossing LED 0 and LED 12 is used to mark the zero degree for microscope calibration. (b) The acquired rubber band image. (c) The binarized image by our thresholding scheme. (d) Perform the convex hull processing to the binary image and adjust the microscope to zero degree of rubber band angle for alignment.

Fig. 17 Some recognition results of 4-band resistors from the set listed in Table 5**.**

Fig. 18 Some recognition results of 5-band resistors from the set listed in Table 6**.**

Fig. 19 Relationship between factor j and SNR of the adopted thresholding expression, where $j = 3.6\times10^{-3}$ is suggested and used in our current study.

Table 1 Mapping a resistor color band into color code, multiplier, and tolerance. Here "-" denotes "Not Available".

Table 2 Several types of light sources used to investigate the effects of specular reflection and halo in resistor recognition. They are displayed respectively in Fig. 15. The 4-band resistor with orange-black-brown-gold color bands and the 5-band resistor with green-white-black-red-brown color ones are used for evaluations. Here "∞" represents that no noisy pixels found in the case, and "NA" represents that the segmentation of color bands fails due to the severe specular reflection.

Table 3 LI analysis corresponding to SNR and recognition results by a brown-red-orange-gold resistor image.

Table 4 LI analysis corresponding to SNR and recognition results by a blue-gray-black-silver-brown resistor image.

Table 5 Results by 10 types of 4-band resistors. Each type contains 20 resistors. The errors result from horizontal alignment, color band extraction, color identification, and color code sequence flip over checking are reported by failed numbers. The total number of failed recognition is 14, and thus the recognition rate is 93%.

Table 6 Results by 10 types of 5-band resistors. Each type contains 20 resistors. The errors result from horizontal alignment, color band extraction, color identification, and color code sequence flip over checking are reported by failed numbers. The total number of failed recognition is 24, and thus the recognition rate is 88%.

Table 7 Simple SNR comparison among Niblack[15], NICK[17] and our method (with $j = 3.6\times10^{-3}$) for binarizing a brown-red-orange-gold resistor image.